Geothermal Resources Council Transactions, Vol. 24, September 24-27, 2000

Numerical Simulation of Non-Darcy Flow in Porous and Fractured Media

Yu-Shu Wu

Earth Sciences Division
Lawrence Berkeley National Laboratory
Berkeley CA 94720

ABSTRACT

A numerical as well as a theoretical study of non-Darcy fluid flow through porous and fractured reservoirs is described. The non-Darcy flow is modeled using a three-dimensional, multiphase flow reservoir simulator. The model formulation incorporates the *Forchheimer* equation which describes non-Darcy flow of both single- or multi-phase fluids in porous media.

The numerical approach is then used to obtain insight into the physics of non-Darcy flow behavior in porous and fractured reservoirs. Several type curves are provided for well-test analyses of non-Darcy flow, which demonstrates the methodology and its application to modeling this type of flow in porous and fractured rocks, including flow in geothermal reservoirs.

Introduction

Darcy's Law, describing a linear relationship between volumetric flow rate (Darcy velocity) and pressure (head or potential) gradient, has been the fundamental principle in flow and transport processes in porous media (Muskat, 1946). Any deviations from this linear relation may be defined as non-Darcy flow. Here, our interest is only in non-Darcy flow caused by high flow velocities. Even though Darcy's Law has been used nearly exclusively in the study of porous-medium phenomena, there is considerable evidence that high-velocity, non-Darcy flow occurs in many subsurface systems, especially in regions near production and injection wells.

The effects of non-Darcy or high-velocity flow regimes in porous media have been observed and investigated for decades (e.g., Tek et al., 1962; Scheidegger, 1972; Katz and Lee, 1990). However, theoretical, field and experimental studies performed so far on these flow regimes have focused mostly on single-phase flow conditions that pertain to the oil and gas industry (Tek et al., 1962; Swift and Kiel, 1962; Lee et al., 1987). Some investigations have been conducted on non-Darcy flow in fractured reservoirs (Skjetne et al., 1999) and into production wells drilled in highly permeable fractured formations (Guppy et al., 1981, 1982). Other studies have concentrated on finding and validating correlations of non-Darcy flow coefficients (Liu et al., 1995).

In the studies of non-Darcy flow through porous media the *Forchheimer* equation (Katz and Lee, 1990) for single-phase flow, is generally used. Several studies reported in the literature extend the *Forchheimer* equation to multiphase flow and provide equations for correlating non-Darcy flow coefficients under multiphase conditions (*Evans et al.*, 1987; *Evans and Evans*, 1988; *Liu et al.*, 1995). A recent study (*Wang* and *Mohanty*, 1999) discusses the importance of multiphase non-Darcy flow in gas-condensate reservoirs and presents a pore-scale network model for these conditions. Because this topic has not been studied in sufficient detail, and due to the difficulty in handling highly nonlinear, non-Darcy flow terms in multiphase flow equations, our understanding non-Darcy flow through permeable (porous and fractured) media is very limited.

The objective of this study is to develop a numerical method for modeling single- and multi-phase, non-Darcy flow through heterogeneous porous and fractured rocks. The model formulation incorporates the *Forchheimer* equation, based on an integral finite-difference or a control volume numerical discretization scheme (Forsyth et al., 1995). The model is implemented into a three-dimensional, three-phase flow numerical simulator, which is applicable to both porous and fractured rocks. For flow in a fractured medium, fracture-matrix interactions are handled using a dual-continua approach, such as double- or multiple-porosity, or dual-permeability methods.

This paper discusses the model formulation and the numerical schemes implemented for modeling non-Darcy flow in porous and fractured media. As application examples, numerical solutions are used to obtain some insight into the physics of flow involving non-Darcy flow effects in reservoirs. Furthermore, several type curves are provided to analyze well test data when non-Darcy flow occurs in porous or fractured rocks.

Governing Equations

It is assumed that a multiphase system in a porous or fractured reservoir is composed of three phases: NAPL (oil), gas (air), and water. For simplicity, the three fluid components, water, NAPL, and gas, are assumed to be present only in their associated phases. Each phase flows in response to pressure, gravitational, and capillary forces according to the multiphase extension of Darcy's law for Darcy flow and the *Forchheimer* equation for non-Darcy flow. In an isothermal system containing three mass components, three mass-balance equations are needed to fully describe the system. For an arbitrary flow of phase f (f = w for water, f = n for NAPL or oil, and f = g for gas) in a porous or fractured domain,

$$\frac{\partial}{\partial t}(\phi\, S_f\, \rho_f) = -\nabla \bullet (\rho_f v_f) + q_f \tag{1}$$

where ϕ is the effective porosity of the formation; ρ_f is the density of fluid f; v_f is the volumetric flow velocity (or normally Darcy velocity) of fluid f; S_f is the saturation of fluid f; t is time; and q_f is the sink/source term of phase (component) f per unit volume of formation.

Volumetric flow velocity (namely Darcy velocity for Darcy flow) for non-Darcy flow of each fluid may be described using the multiphase extension of *Forchheimer* equation (Evans and Evans, 1988; Liu et al., 1995):

$$-(\nabla P_f - \rho_f g) = \frac{\mu_f}{k k_{rf}} v_f + \beta_f \rho_f v_f |v_f| \tag{2}$$

where P_f is the pressure of phase f; g is the gravitational constant vector; k is the absolute/intrinsic permeability (tensor) of the formation; k_{rf} is relative permeability to phase f; and β_f is the effective non-Darcy flow coefficient with a unit m^{-1} for fluid f under multiphase flow conditions (Evans and Evans, 1988).

Equation (2) implicitly defines the Darcy velocity as a function of pressure gradient as well as saturation and relative permeability. A more general relation for the Darcy velocity in multiphase, non-Darcy flow may be proposed as a function of pressure gradient, saturation, and relative permeability functions

$$v_f = v_f\left(\nabla P_f, S_f, k_{rf}\right) \tag{3}$$

Equation (3) can extend many other kinds of equations for non-Darcy flow, in addition to the *Forchheimer* equation (e.g., Scheidegger, 1972), to describing multiphase, non-Darcy flow conditions.

Equation (1), governing mass balance for three phases, needs to be supplemented with constitutive equations, which express all the secondary variables and parameters as functions of a set of primary thermodynamic variables of interest. The following relationships will be used to complete the description of multiphase flow through porous and fractured media

$$S_w + S_n + S_g = 1 \tag{4}$$

Capillary pressures relate pressures between the different phases. The aqueous- and gas-phase pressures are related as

$$P_w = P_g - P_{cgw}\left(S_w\right) \tag{5}$$

where P_{cgw} is the gas-water capillary pressure in a three-phase system and assumed to be a function of water saturation only. The NAPL pressure is related to the gas phase pressure by

$$P_n = P_g - P_{cgn}\left(S_w,\ S_n\right) \tag{6}$$

where P_{cgn} is the gas-NAPL capillary pressure in a three-phase system, which is a function of both water and NAPL saturations. For many reservoir rocks, the wettability order is (1) aqueous phase, (2) NAPL phase, and (3) gas phase. The gas-water capillary pressure is usually stronger than the one between gas and NAPL . In a three-phase system, the NAPL-water capillary pressure, P_{cnw}, may be defined as

$$P_{cnw} = P_{cgw} - P_{cgn} = P_n - P_w \tag{7}$$

The relative permeabilities are assumed to be functions of fluid saturations only. The relative permeability to the water phase is described by

$$k_{rw} = k_{rw}\left(S_w\right) \tag{8}$$

to the NAPL phase by

$$k_{rn} = k_{rn}\left(S_w,\ S_g\right) \tag{9}$$

and to the gas phase by

$$k_{rg} = k_{rg}\left(S_g\right) \tag{10}$$

In general, the densities of water, NAPL, and gas, as well as the viscosities of fluids, can be treated as functions of fluid pressures.

Numerical Formulation

The multiphase non-Darcy flow equations, as discussed in the previous section, have been implemented into a general-purpose, three-phase reservoir simulator, the MSFLOW code (Wu, 1998). As implemented in the code, Equation (1) can be discretized in space using an integral finite-difference or control-volume finite-element scheme (Pruess, 1991) for a porous and/or fractured medium. The time discretization is carried out with a backward, first-order, finite-difference scheme. The discrete nonlinear equations for water, NAPL, and gas flow at Node i are written as follows

$$\left\{(\phi\, S_f \rho_f)_i^{n+1} - (\phi\, S_f \rho_f)_i^{n}\right\}\frac{V_i}{\Delta t} = \sum_{j\in\eta_i}(F_f)_{ij}^{n+1} + Q_{fi}^{n+1} \tag{11}$$

where n denotes the previous time level; n+1 is the current time level; V_i is the volume of element i (porous or fractured block); Δt is the time step size; η_i contains the set of neighboring elements (j), porous or fractured block, to which element i is directly connected; and F_f is a mass flow term between elements i and j, defined [when Equation (2) is used] as

$$F_f = \frac{A_{ij}}{2(k\beta_f)_{ij+1/2}} \left\{ -\frac{1}{\lambda_f} + \left[\left(\frac{1}{\lambda_f} \right)^2 - \gamma_{ij} \left(\psi_{fj} - \psi_{fi} \right) \right]^{1/2} \right\} \qquad (12)$$

where subscript ij+1/2 denotes a proper averaging of properties at the interface between the two elements and A_{ij} is the common interface area between connected elements i and j. The mobility of phase f is defined as

$$\lambda_f = \frac{k_{rf}}{\mu_f} \qquad (13)$$

and the flow potential term is

$$\psi_{fi} = P_{fi} - r_{ij+1/2} g D_i \qquad (14)$$

where D_i is the vertical distance between a datum and the center of element i. The mass sink/source term at element i, Q_{fi} for phase f, is defined as

$$Q_{fi} = q_{fi} V_i \qquad (15)$$

In Equation (12), transmissivity of flow terms is defined (if the integral finite-difference scheme is used) as,

$$\gamma_{ij} = \frac{4\left(k^2 \rho_f \beta_f\right)_{ij+1/2}}{d_i + d_j}, \qquad (16)$$

where d_i is the distance from the center of element i to the interface between elements i and j.

In the model formulation, absolute and relative permeabilities, and effective non-Darcy flow coefficient are all considered as flow properties of the permeable medium and need to be averaged between connected elements in calculating the mass flow terms. In general, weighting approaches used are that absolute permeability is harmonically weighted along the connection between elements i and j; relative permeability and non-Darcy flow coefficients are both upstream weighted.

Newton/Raphson iterations are used to solve Equation (11). For a three-phase flow system, 3 × N coupled, nonlinear equations must be solved (N being the total number of elements of the grid), including three equations at each element for the three mass-balance equations for water, NAPL, and gas, respectively. The three primary variables (x_1, x_2, x_3) selected for each element are gas pressure, gas saturation, and NAPL saturation, respectively. In terms of the three primary variables, the Newton/Raphson scheme gives rise to

$$\sum_m \frac{\partial R_i^{\beta,n+1}\left(x_{m,p}\right)}{\partial x_m} \left(\delta x_{m,p+1}\right) = -R_i^{\beta,n+1}\left(x_{m,p}\right)$$

$$\textit{for } m = 1, 2, \textit{ and } 3 \qquad (17)$$

where index m = 1, 2, and 3 indicates the primary variable 1, 2, or 3, respectively; p is the iteration level; and i = 1, 2, 3, ..., N, the nodal index. The primary variables are updated after each iteration; that is,

$$x_{m,p+1} = x_{m,p} + \delta x_{m,p+1} \qquad (18)$$

A numerical method is used to construct the Jacobian matrix for Equation (17), as outlined by Forsyth et al. (1995).

Applications and Discussion

In this section, we present two application examples and discuss single-phase, non-Darcy flow behavior to demonstrate the applicability of the present modeling approach to field problems. The examples generate dimensionless pressures or type curves for non-Darcy flow well test analyses, including (1) Pressure drawdown and buildup analyses, and (2) Pressure drawdown in fractured reservoirs

Before further discussing these application problems, we introduce several dimensionless variables for analyzing single-phase flow and well test results (Earlougher, 1977). Let us define the following group of dimensionless variables

The dimensionless radius

$$r_D = \frac{r}{r_w} \qquad (19)$$

the dimensionless time,

$$t_D = \frac{kt}{\phi_i \mu C_t r_w^2} \qquad (20)$$

the dimensionless non-Darcy flow coefficient

$$\beta_D = \frac{k q_m b}{2\pi r_w h \mu} \qquad (21)$$

and the dimensionless pressure

$$P_D = \frac{P_i - P}{\dfrac{q_v \mu}{2\pi k h}} \qquad (22)$$

In these notations, the subscript referring to a phase is ignored; r is radial distance (coordinate), r_w is wellbore radius, ϕ_i is the effective (or initial) porosity of the reservoir at reference (initial) pressure ($P = P_i$), C_t is total compressibility of fluid and rock, h is thickness of formation, q_m is mass production or injection rate, and q_v is volumetric production or injection rate.

Pressure Drawdown and Buildup Analyses

This example presents a set of type curves for analyzing well tests of single-phase, slightly compressible, non-Darcy fluid flow in an infinite-acting reservoir. The basic modeling parameters are summarized in Table 1. Non-Darcy flow is considered to occur into a fully penetrating well from an infinite-acting, homogeneous and isotropic, uniform and horizontal formation.

Even though here skin and wellbore storage effects are ignored in the results, they can easily be included in the analysis.

In the numerical model the infinite-acting reservoir is approximated by a one-dimensional, radially symmetrical reservoir with an outer boundary radius of 5×10^6 (m), discretized into a one-dimensional grid of 3,100 gridblocks based on a logarithmic scale. Initially, the system is undisturbed and at constant pressure. A fully penetrating injection well, represented by a well element, starts producing at a specified constant rate at time t = 0.

Table 1. Parameters for the pressure drawdown and buildup analysis.

Parameter	Value	Unit
Initial Pressure	$P_i = 10$	Bar
Initial Porosity	$\phi_i = 0.20$	
Reference Fluid Density	$\rho_i = 1{,}000$	kg/m³
Formation Thickness	h=10	m
Fluid Viscosity	$\mu = 1 \times 10^{-3}$	Pa•s
Fluid Compressibility	$C_f = 5 \times 10^{-10}$	Pa⁻¹
Rock Compressibility	$C_r = 5 \times 10^{-9}$	Pa⁻¹
Permeability	$k = 9.869 \times 10^{-13}$	m²
Water Injection Rate	$q_v = 0.1$	m³/d
Wellbore Radius	$r_w = 0.1$	m
Outer Boundary Radius	$r_e = \infty \approx 5 \times 10^6$	m
Dimensionless non-Darcy Flow Coefficient	$\beta_D = 1 \times 10^{-3}$, 1, 10, 100 1×10^3, 1×10^4, 1×10^5	

A set of type-curves for pressure drawdown, calculated by the numerical model in terms of dimensionless pressure versus dimensionless time, is shown in Figure 1. The results clearly indicate that the non-Darcy flow coefficient is a very important and sensitive parameter to the pressure drawdown curves. When non-Darcy flow coefficients are sufficiently large, they affect pressure transient behavior during both earlier and later times. Note that in the simulation, the non-Darcy flow coefficient is treated to be uncorrelated with other parameters. Figure 1 indicates that the non-Darcy flow coefficient can be effectively estimated using the type curves following the traditional type-curve matching approach. Note also that for small coefficients, pressure declines at the well during production are approaching those predicted by the Theis solution, as it should be.

Figure 2 presents simulated pressure drawdown and buildup curves, in which the well is pumped for only one day and then shut in. As shown in the figure, the well pressure variations during the entire production and shut-in period indicate that pressure buildup is insensitive to the values of non-Darcy flow coefficients, as compared with drawdown during production. This is because after the well is shut in, flow velocities near the wellbore are significantly reduced, and non-Darcy flow effects become negligible. Many additional modeling investigations have confirmed this observation. It indicates that pressure-buildup tests are not suitable for estimating non-Darcy flow coefficients. On the other hand, the pressure-buildup method, following non-Darcy flow production tests, will be a good test for determining permeability values without significant non-Darcy flow.

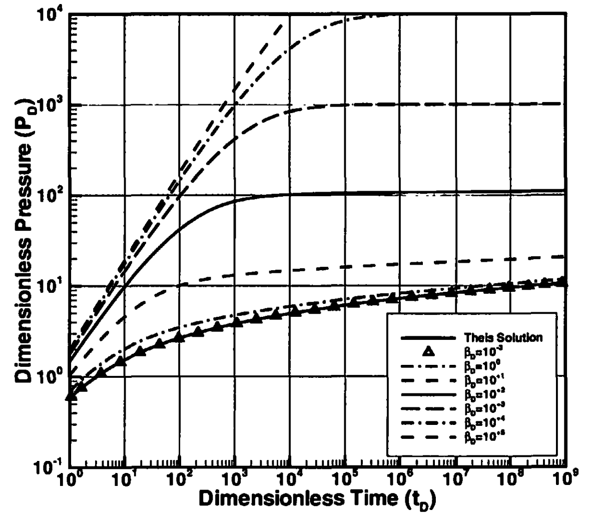

Figure 1. Type curves for dimensionless pressures for non-Darcy flow

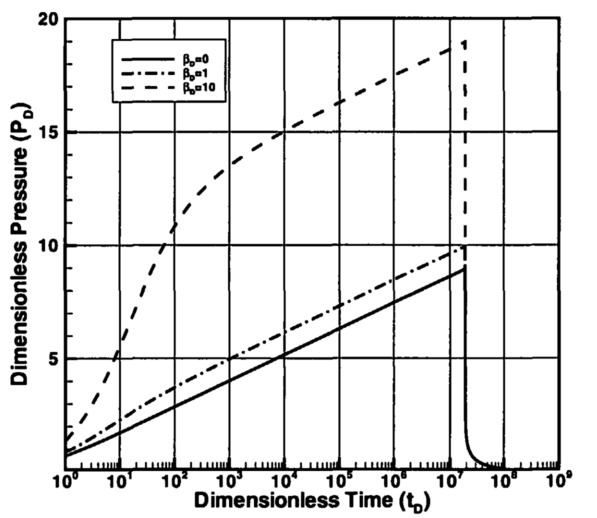

Figure 2. Dimensionless pressures for one-day production, followed by pressure buildup, of non-Darcy flow in an infinite system assuming no wellbore storage and skin effects.

Analysis of non-Darcy Flow in Fractured Media

In this part of the study, the fracture-matrix formation is described using the Warren and Root (1963) double-porosity model. The physical flow model is a one-dimensional fracture-matrix system, whose basic rock and fluid properties are given in Table 2.

A radially symmetrical reservoir ($r = 5 \times 10^6$ m) is discretized into a one-dimensional (r), primary grid. The radial distance is subdivided into 3,100 intervals based on a logarithmic scale. A double-porosity mesh is generated from the primary grid, in which a three-dimensional fracture network and cubic matrix blocks are used. The matrix block size is $1 \times 1 \times 1$ meter, and fracture permeability and aperture are correlated by the cubic law. Note that in the matrix domain ten-times larger non-Darcy flow coefficients than those for the fractures are used, to account for lower matrix permeability and high non-Darcy flow effects. A fully penetrating production well is represented by a well element with a specified constant production rate.

Table 2. Parameters for the single-phase, fractured-medium flow problem.

Parameter	Value	Unit
Matrix Porosity	$\phi_M = 0.30$	
Fracture Porosity	$\phi_F = 0.0006$	
Reference Water Density	$\rho_w = 1{,}000$	kg/m³
Water Phase Viscosity	$\mu_w = 1\times10^{-3}$	Pa•s
Matrix Permeability	$k_M = 1.0\times10^{-16}$	m²
Fracture Permeability	$k_F = 9.869\times10^{-13}$	m²
Water Production Rate	$q_m = 0.1$	kg/s
Rock Compressibility	$C_r = 1.0\times10^{-9}$	1/Pa
Water Compressibility	$C_w = 5.0\times10^{-10}$	1/Pa
Dimensionless non-Darcy Flow Coefficient for fracture	$\beta D, f = 1 \times 10^{-4}$, 1, 5, and 10	
Dimensionless non-Darcy Flow Coefficient for matrix	$\beta D, m = 1\times 10^{-3}$, 10, 50, and 100	
Wellbore Radius	$r_w = 0.1$	m

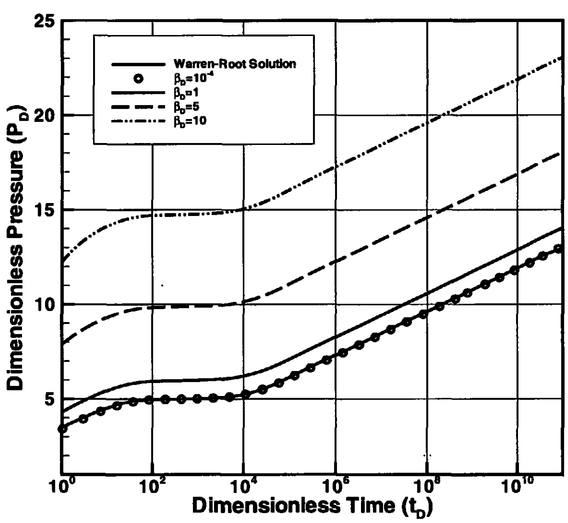

Figure 3. Type curves for dimensionless pressures for non-Darcy flow in an infinite fractured system assuming no wellbore storage and skin effects (dimensionless non-Darcy flow coefficients for fracture systems).

For non-Darcy flow into a well from an infinite fractured system, well pressures type curves using semi-log plots are given in Figure 3. These type curves show that well (fracture) pressures are extremely sensitive to the value of non-Darcy flow coefficients. Therefore, well production tests will help determine these coefficients in a fractured reservoir. Furthermore, Figure 3 indicates that the effects of non-Darcy flow on early transient pressure responses are very strong, such that the first semi-log straight lines may not develop when non-Darcy flow is involved.

Summary and Conclusions

This paper presents a numerical method and theoretical study of non-Darcy flow through porous and fractured media. A three-dimensional, three-phase flow reservoir simulator has been enhanced to include the capability of modeling non-Darcy flow. Model formulation incorporates the *Forchheimer* equation to describe single-phase and multiphase non-Darcy flow. As application examples, numerical solutions are used to obtain some insight into the physics of flow involving non-Darcy flow effects in porous media. It has been found that pressure drawdown not buildup behavior is sensitive to effects of non-Darcy flow. Therefore pressure drawdown testing will be a suitable approach to determine non-Darcy flow coefficients. In addition, several type curves are provided for well test analyses of non-Darcy flow to demonstrate the usefulness of the proposed methodology for investigating non-Darcy flow in porous and fractured rocks.

Acknowledgements

The author is indebted to J. Liu, M. Lippmann and D. Hawkes for their careful and critical review of this manuscript. This work was supported in part by the Assistant Secretary for Energy Efficiency and Renewable Energy, Office of Geothermal and Wind Technologies of the U.S. Department of Energy, under Contract No. DE-AC03-76SF00098.

References

Earlougher, R. C. Jr., 1977, *Advances in Well Test Analysis*, SPE Monograph, Vol. 5, SPE of AIME, Dallas.

Evans, E. V. and Evans, R. D., 1988, Influence of an immobile or mobile saturation on non-Darcy compressible flow of real gases in propped fractures, *J. Petroleum Technology*, Vol. 40, No. 10, 1343-1351.

Evans, R. D., Hudson, C. S. and Greenlee, J. E., 1987, The effect of an immobile liquid saturation on the non-Darcy flow coefficient in porous media, *J. SPE Production Engineering, Trans.* AIME, Vol. 283, 331-338.

Forsyth, P. A., Wu, Y. S. and Pruess, K., 1995, Robust numerical methods for saturated-unsaturated flow with dry initial conditions in heterogeneous media, *Advances in Water Resources*, Vol. 18, pp. 25-38.

Guppy, K., Cinco-Ley, H., H. and Ramey, H. J. Jr., *1981,* Effects of non-Darcy flow on the constant-pressure production of fractured wells, *Soc. Pet. Eng. J., June, 390-400.*

Guppy, K., Cinco-Ley, H., H., Ramey, H. J. Jr. and Samaniego, F., *1982,* Non-Darcy flow in wells with finite-conductivity vertical fractures, *Soc. Pet. Eng. J., October, 681-698.*

Katz, D. L. and Lee, R. L., 1990, *Natural Gas Engineering, Production and Storage*, Chemical Engineering Series, McGraw-Hill Book Co. Inc., New York.

Lee, R. L., Logan, R. W. and Tek, M. R., 1987, "Effetcs of turbulence on transient flow of real gas through porous media," *SPE Formation Evaluation*, March, 108-120.

Liu, X., Civan, F. and Evans, R. D., 1995, Correlations of the non-Darcy flow coefficient, *J. Canadian Petroleum Technology,* Vol. 34, No. 10, 50-54.

Muskat, M., 1946, *The Flow of Homogeneous Fluids through Porous Media*, J. W. Edwards, Inc., Ann Arbor, Michigan.

Pruess, K., 1991, TOUGH2 - A General-Purpose Numerical simulator for multiphase fluid and heat flow, Report LBL-29400, Lawrence Berkeley National Laboratory, Berkeley, California.

Scheidegger, A. E., *1972, The Physics of Flow through Porous Media, University of Toronto Press.*

Skjetne, E., Statoil, T. K. and Gudmundsson, J. S., 1999, Experiments and modeling of high-velocity pressure loss in sandstone fractures, SPE 56414, Presented at the 1999 SPE Annual Technical Conference and Exhibition, Houston, Texas.

Swift, G. W. and Kiel, O. G., 1962, The prediction of gas-well performance including the effects of non-Darcy flow, *J. Petroleum Technology, Trans.* AIME, Vol. 222, 791-798.

Tek, M. R., Coats, K. H. and Katz, D. L., 1962, The effects of turbulence on flow of natural gas through porous reservoirs, *J. Petroleum Technology, Tran.s* AIME, Vol. 222, 799-806.

Wang, X. and Mohanty, K. K., 1999, Multiphase non-Darcy flow in gas-condensate reservoirs, SPE 56486, Presented at the 1999 SPE Annual Technical Conference and Exhibition, Houston, Texas.

Warren, J.E. and Root, P. J., 1963, The behavior of naturally fractured reservoirs, *Soc. Pet. Eng. J., Trans., AIME*, Vo. 228, 245-255.

Wu, Y. S., 1998, MSFLOW: *Multiphase Subsurface Flow Model of Oil, Gas and Water in Porous and Fractured Media with Water Shut-off Capability, Documentation and User's Guide*, Research Report, 841 LeRoy Lane, Walnut Creek, California.